ISSN 1674-1056
http://cpb.iphy.ac.cn
http://iopscience.iop.org/cpb
中国物理 B
Chinese Physics
中国物理 Chinese Physics B

Discovery of superhard materials via CALYPSO methodology

Shuangshuang Zhang(张爽爽), Julong He(何巨龙), Zhisheng Zhao(赵智胜), Dongli Yu(于栋利), Yongjun Tian(田永君)

Citation: Chin. Phys. B . 2019, 28(10): 106104 . **doi:** 10.1088/1674-1056/ab4179
Journal homepage: http://cpb.iphy.ac.cn; http://iopscience.iop.org/cpb

What follows is a list of articles you may be interested in

The CALYPSO methodology for structure prediction

Qunchao Tong(童群超), Jian Lv(吕健), Pengyue Gao(高朋越), Yanchao Wang(王彦超)
Chin. Phys. B . 2019, 28(10): 106105 . **doi:** 10.1088/1674-1056/ab4174

Isostructural phase transition-induced bulk modulus multiplication in dopant-stabilized ZrO_2 solid solution

Min Wang(王敏), Wen-Shu Shen(沈文舒), Xiao-Dong Li(李晓东), Yan-Chun Li(李延春), Guo-Zhao Zhang(张国召), Cai-Long Liu(刘才龙), Lin Zhao(赵琳), Shu-Peng Lv(吕舒鹏), Chun-Xiao Gao(高春晓), Yong-Hao Han(韩永昊)
Chin. Phys. B . 2019, 28(7): 076109 . **doi:** 10.1088/1674-1056/28/7/076109

First-principles calculations of structure and elasticity of hydrous fayalite under high pressure

Chuan-Yu Zhang(张传瑜), Xu-Ben Wang(王绪本), Xiao-Feng Zhao(赵晓凤), Xing-Run Chen(陈星润), You Yu(虞游), Xiao-Feng Tian(田晓峰)
Chin. Phys. B . 2017, 26(12): 126103 . **doi:** 10.1088/1674-1056/26/12/126103

Influence of Tb on easy magnetization direction and magnetostriction of ferromagnetic Laves phase $GdFe_2$compounds

Adil Murtaza, Sen Yang(杨森), Chao Zhou(周超), Xiaoping Song(宋晓平)
Chin. Phys. B . 2016, 25(9): 096107 . **doi:** 10.1088/1674-1056/25/9/096107

Theoretical design of diamondlike superhard structures at high pressure

Quan Li(李全), Wei-Tao Zheng(郑伟涛)
Chin. Phys. B . 2016, 25(7): 076103 . **doi:** 10.1088/1674-1056/25/7/076103

TOPICAL REVIEW — CALYPSO structure prediction methodology and its applications to materials discovery

Discovery of superhard materials via CALYPSO methodology*

Shuangshuang Zhang(张爽爽), Julong He(何巨龙), Zhisheng Zhao(赵智胜)†, Dongli Yu(于栋利), and Yongjun Tian(田永君)

Center for High Pressure Science (CHiPS), State Key Laboratory of Metastable Materials Science and Technology, Yanshan University, Qinhuangdao 066004, *China*

(Received 30 June 2019; revised manuscript received 3 September 2019; published online 30 September 2019)

The study of superhard materials plays a critical role in modern industrial applications due to their widespread applications as cutting tools, abrasives, exploitation drills, and coatings. The search for new superhard materials with superior performance remains a hot topic and is mainly considered as two classes of materials: (i) the light-element compounds in the B–C–N–O(–Si) system with strong and short covalent bonds, and (ii) the transition-element light-element compounds with strong covalent bonds frameworks and high valence electron density. In this paper, we review the recent achievements in the prediction of superhard materials mostly using the advanced CALYPSO methodology. A number of novel, superhard crystals of light-element compounds and transition-metal borides, carbides, and nitrides have been theoretically identified and some of them account well for the experimentally mysterious phases. To design superhard materials via CALYPSO methodology is independent of any known structural and experimental data, resulting in many remarkable structures accelerating the development of new superhard materials.

Keywords: CALYPSO, superhard materials, crystal structure, prediction

PACS: 61.50.Ah, 61.50.Ks, 31.15.A– **DOI:** 10.1088/1674-1056/ab4179

1. Introduction

Superhard materials have been widely used in industrial operations due to their superior hardness, incompressibility, and wear resistance compared with other materials. The synthesis of diamond and cubic boron nitride (cBN) has led to the development of superhard materials and multiple related disciplines.[1,2] Diamond has been considered as the hardest, stiffest, and most incompressible substance in nature, but it has poor thermal stability and reactivity with ferrous alloys. Although cBN has been considered as the more optimal candidate for cutting ferrous and carbide-forming hard substances compared with diamond, the hardness of cBN single crystal is only half of that of diamond crystal. Therefore, the discovery of novel superhard materials with combined superior mechanical performance and high stability is of great interest.

Superhard materials are exclusively covalent compounds because short and strong covalent bonds highly resist both elastic and plastic deformations.[3] The light elements (LE), including B, C, N, and O, etc., have a strong ability to form covalent bonds, making their compounds potential candidates.[4–6] In the past decades, superhard carbon phases and carbon nitrides, diamond-like boron carbides (*d*-BC_x[7–9]) and boron carbonitrides (*d*-BC_xN[10–14]), elemental boron allotropes,[15–17] boron-rich compounds (e.g., B_6O,[18] $B_{13}C_2$,[19] and B_4C[8]), boron carbon oxide (e.g., B_2CO[20,21] and B_2C_xO[22]), and boron nitrogen oxide (e.g., B_3NO[23]), have all been extensively explored both experimentally and theoretically. Outstanding structures among these materials are sp^3 or sp^3-rich carbon phases with extremely high hardness compared with that of diamond crystal.[24–30] It is reasonable to suppose that pure covalent C–C bonds provide such materials with remarkable hardness. Compared with the pure covalent bond in diamond, the significant ionicity (0.256) of the B–N bond limits the hardness of cBN crystal to approximately half that of diamond. Therefore, the material with superior hardness than diamond crystal may be difficult to find in the B–C–N–O(–Si) system due to its existing ionicity. For example, the hardness values of diamond-like BC_5, BC_2N, and BC_4N were reported to be 71,[8] 76,[10] and 68 GPa,[31] respectively, which were less than that of diamond but exceeded that of *c*-BN. Nevertheless, other anticipated electrical and thermal properties were found in these polar covalent crystals. For example, the thermal stabilities of *d*-BC_x[8] and *d*-BC_xN[32] under inert conditions were higher than that of diamond. Moreover, peculiar electronic properties, including semi-conductivity or even superconductivity, were found in *d*-BC_x and B_2CN materials.[33,34]

In the search for new superhard materials, researchers have focused on transition-metal light-element (TM-LE) com-

*Project supported by the National Key Research and Development Program of China (Grant No. 2018YFA0703400), the National Natural Science Foundation of China (Grant Nos. 51722209, 51572235, and 51672238), the 100 Talents Plan of Hebei Province of China (Grant No. E2016100013), the NSF for Distinguished Young Scholars of Hebei Province of China (Grant No. E2018203349), and the Key Research and Development Program of Hebei Province of China (Grant No. 17211110D).

†Corresponding author. E-mail: zzhao@ysu.edu.cn

© 2019 Chinese Physical Society and IOP Publishing Ltd

pounds because of their high valence electron densities and strong covalent bonding frameworks. However, these compounds are mostly metallic — a property that has an obvious negative effect on their hardness. For example, transition metal (TM) borides (e.g., WB_4) commonly have hardness values of 20–30 GPa.[35] Past studies have identified that the synthesized c-Zr_3N_4 possessed unique semiconducting property, leading to a hardness value of as high as 36 GPa.[36] In addition, the semiconducting pyrite-type PtN_2 had been predicted to be a superhard material with theoretical hardness of 60 GPa.[37] Thus, the exploration of semiconducting superhard materials in TM-LE systems is highly promising.

The theoretical design of new materials is gaining broad recognition as an effective means of reducing the number of experiments that can ultimately lead to material discovery. In such a context, several efficient structure prediction methods have been proposed and applied to explore new materials, including simulated annealing,[38] genetic algorithms,[39,40] minima hopping,[41] basin hopping,[42] random sampling,[43] and CALYPSO.[44,45] Their computational structures not only added fresh blood to the material family, but also solved many experimental indeterminate phases. For example, the proposed hypothetical carbon phases of M-carbon,[46] bct-C_4,[27] F-carbon,[47] W-carbon,[48] and O-carbon[49] have been considered as the structural solution to cold-compressed graphite phases.[47,50,51] Indeed, it was difficult to determine the exact stoichiometric ratios and atomic positions of LE compounds in experiments because of their low diffraction intensity and close atomic number. Furthermore, the large difference in atomic mass between TM and LE also served as a major obstacle in determining their composition and LE position. In relation to the above mentioned, structure prediction provides a powerful approach for clarifying the structures of experimentally discovered phases. For instance, new compounds of boron carbides, including BC_3 and BC_5, have been claimed to be synthesized, but their exact structures are difficult to determine in the experiments.[8,9,51] Various structures of diamond-like BC_5, such as tetragonal BC_5,[53] hexagonal BC_5-2,[54] and orthorhombic BC_5,[55] were predicted to match the experimental XRD and Raman results. For the TM-LE compounds, for example, the structure of experimentally synthesized Re_2C was determined by combining the experimental results with first-principle calculations.[56] Noticeably, the current wide applications of structure prediction have helped to understand experimentally discovered novel phases, and CALYPSO as one of the most distinguished structure prediction methods has been proven useful in solving complex crystal structures and in designing novel functional materials, such as superhard, superconducting, and semiconducting materials.[57–65]

Here, we focus on recent advances in the design of superhard materials mainly based on the structure prediction of CALYPSO methodology. Its basic theory and general features are introduced first, followed by examples of recent applications of superhard materials among compounds of LE (B, C, N, O, and Si) and TM borides, carbides, and oxides. Finally, the current challenges and future expectations in designing superhard materials through structure prediction methods are summarize.

2. CALYPSO methodology

CALYPSO, one of the advanced structural prediction methods, has been widely applied in the design of various structural materials, including three-dimensional (3D) bulk structures, two-dimensional (2D) surfaces and layers, and isolated clusters or molecules, with a variety of functional properties.[59,60,63–70] The particle swarm optimization (PSO) technique algorithm was adopted as implemented in the CALYPSO code for structure prediction on the basis of an efficient global minimization of free-energy surfaces merging *ab initio* total-energy calculations. Compared with the previous data mining method, CALYPSO requires only chemical compositions for a given compound to predict structures under given external conditions (e.g., pressure) without the need of any prior known structural information about unit cell size, shape, and atomic positions.[45,57,71] Additionally, a straightforward way by which to design superhard materials has been developed recently based on CALYPSO; this approach integrated structure searching, total energy calculations, and theoretical hardness models to readily seek the energetically favorable superhard structures.[61]

3. Discovery of superhard materials by using CALYPSO

The search for new superhard materials has been an important research field in material science. Nowadays, these explorations primarily focus on two classes of materials: (i) the LE compounds in the B–C–N–O(–Si) system with 3D networks of strong covalent bonds, including a number of carbon allotropes, and binary and ternary B–C–N–O(–Si) compounds, and (ii) the TM-LE compounds having high valence electron density, such as FeB_4, WB_3, RhB, Re_2 C, PtN_2, and IrN_2. Using structure prediction, plenty of previously undetectable structures of superhard crystals can be created now, and some of them account well for the experimental problems.

3.1. Light-elements compounds

3.1.1. Carbon polymorphs

The carbon element is fascinating because of the diversified polymorphs profiting from its sp-, sp^2-, and sp^3-hybridized states. For example, graphite, diamond, fullerenes, graphene, carbine, and amorphous carbon exhibit outstanding properties and are of scientific and technological importance.

Therefore, exploring new carbon polymorphs has long been a hot topic in scientific communities.

The sp^3- and high sp^3-hybridized carbons generally have a dense, superhard, and strong nature. Thus, exploring them has become the common way to uncover superhard materials. For example, the predicted all-sp^3 carbons of *Cco*-C_8, *o*C_{32}, and *F*-carbon exhibit extreme hardness values exceeding 90 GPa.[29,30,72] They (Figs. 1(a)–1(c)) contain (4+8+6)-membered or (5+6+7)-membered rings, can be viewed as solutions to the cold-compressed graphite phases.[47,50,51] The cage-like carbons (also called clathrate carbons), a class of low-density superhard sp^3 carbons, can be viewed as carbon cages linked by sp^3 bonds possessing excellent mechanical performance. This is exemplified by the C_{60} clathrate carbon that has a C_{60} cage (Fig. 1(d)) and a *fcc*-C_{32} carbon that has a C_{32} cage (Fig. 1(e)) with hardness values of approximately 82.8 and 79.9 GPa, respectively.[73,74] Significantly, these cage-like structures can also become hosts for superconducting materials. More recent experiments reported a superhydride, LaH_{10}, with a superconducting transition temperature (T_c) close to room temperature[75–77] and a structure reminiscent of the cage-like *fcc*-C_{32} carbon. The *P* carbon (Fig. 1(f)), another relatively low-density superhard sp^3 carbon adopting the microporous framework, is a superhard semiconductor with a direct band gap of 3.12 eV.[78] Regardless of density, all-sp^3 carbons are semiconducting due to the electron localization of sp^3-hybridized C–C bonds, as shown in Table 1.

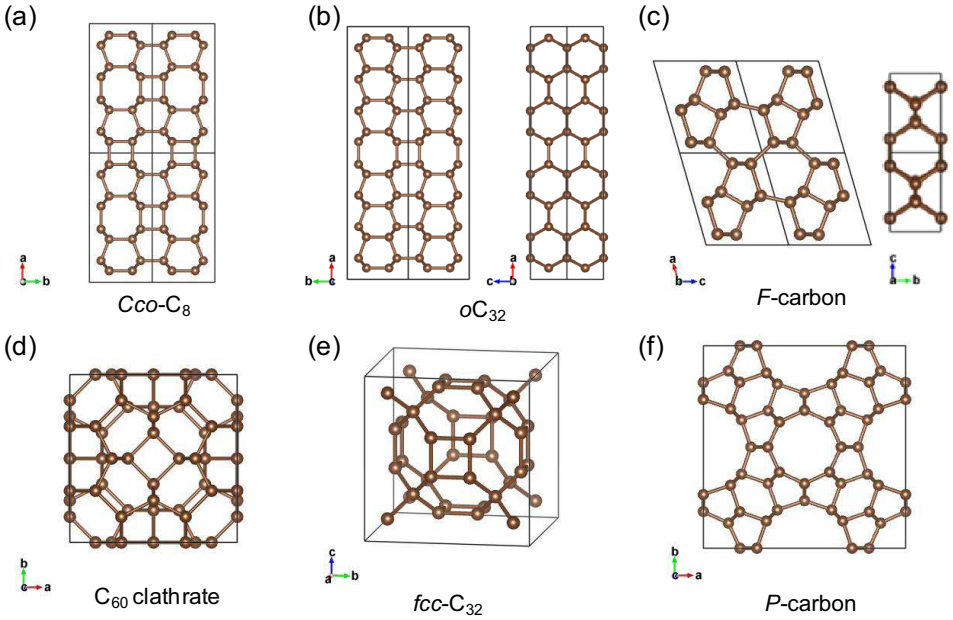


Fig. 1. Predicted crystal structures of superhard sp^3-hybridized carbon allotropes. Both structures in (a) and (b) consist of (4+6+8)-membered rings,[30,72] and the carbon structure in (c) consists of (5+6+7)-membered rings.[29] These structures were viewed as solutions to the experimentally mysterious cold-compressed graphite or carbon nanotubes.[25,47,48] The carbon structures in (d) and (e) contain the unique C_{60} and C_{32} cages, respectively.[73,74] Notably, the predicted fcc-C_{32} (e) has the same structure with recently synthesized LaH_{10} possessing T_c near room temperature at high pressure.[75–77] (f) A type of microporous carbon form.[78]

Table 1. Space group (S.G.), density (g/cm^3), and calculated hardness (H, GPa), bulk modulus (B_0, GPa), B/G ratio, and band gap (E_g, eV) of predicted sp^3-hybridized carbon polymorphs.

Structure	S.G.	Density	H	B	B/G	E_g	Framework	Hybridization	Refs.
Diamond	Fd-3m	3.63	98.2	454.7	0.83	4.2	6-membered rings	sp^3	
Graphite	$P63/mmc$	2.3	/	/	/	metallic	6-membered rings	sp^2	
Cco-C_8	$Cmmm$	3.51	95.1	444.1	0.91	3.12	(4+8+6)-membered rings	sp^3	[30]
oC_{32}	$Cmmm$	3.56	96.2	457	0.88	3	(4+6+8)-membered rings	sp^3	[72]
F-carbon	$P2/m$	3.46	93.9	410.2	0.89	4.55	(5+6+7)-membered rings	sp^3	[29]
C_{60} clathrate	$\mathfrak{I}$-3m	3.34	82.8	392	0.92	2.26	C_{60} cage unit	sp^3	[73]
fcc-C_{32}	Fm-3m	2.75	79.9	457	1.1	2	C_{32} cage unit	sp^3	[74]
P-carbon	$I4/mmm$	3.1	86.7	334.2	0.93	3.52	microporous	sp^3	[78]

Polymerizing various carbon nanotubes is another popular approach to producing superhard carbons. As depicted in Fig. 2 and Table 2, 3D carbon nanotube polymers exhibit abundant structures [i.e., 3D-(n, 0) and 3D-(n, n)], including the sp^3 (4+6+8)-membered 3D-(2, 2), 3D-(3, 0) (lonsdaleite), and a number of different sp^2-sp^3 porous carbons (Fig. 2(a)–2(i)) with the junctions composed of diamond-like sp^3 bonds.[79–81] Further investigations of their mechanical properties show that these polymers have ultrahigh hardness, good ductility, high tensile strength and Young's modulus, and

low density. Contrary to all-sp^3 carbons, these low-density sp^2-sp^3 carbons have specific electrical properties, from semiconductors with tunable band gaps to conductors. According to the internal arrangement of sp^2 atoms, the 1D, 2D, and 3D metallic carbons can be theoretically designed by compressing carbon nanotubes.

The sp-sp^2/sp^3 carbons, including graphyne, graphdiyne, and yne-diamonds (YDs), have been reported both theoretically and experimentally. The calculations indicated that the acetylenic linkages can assemble these 2D carbons into 3D polymers. As a result, these 3D polymers were expected to be a new kind of superhard materials. Under this assumption, several graphyne, graphdiyne, and yne-diamond polymers were theoretically designed recently (Figs. 2(j)–2(l)) and were observed to have superior properties, including ultrahigh hardness and tunable band gaps.[82–84] These findings are likely to be useful in guiding the design and synthesis of superhard carbon materials with novel electrical properties.

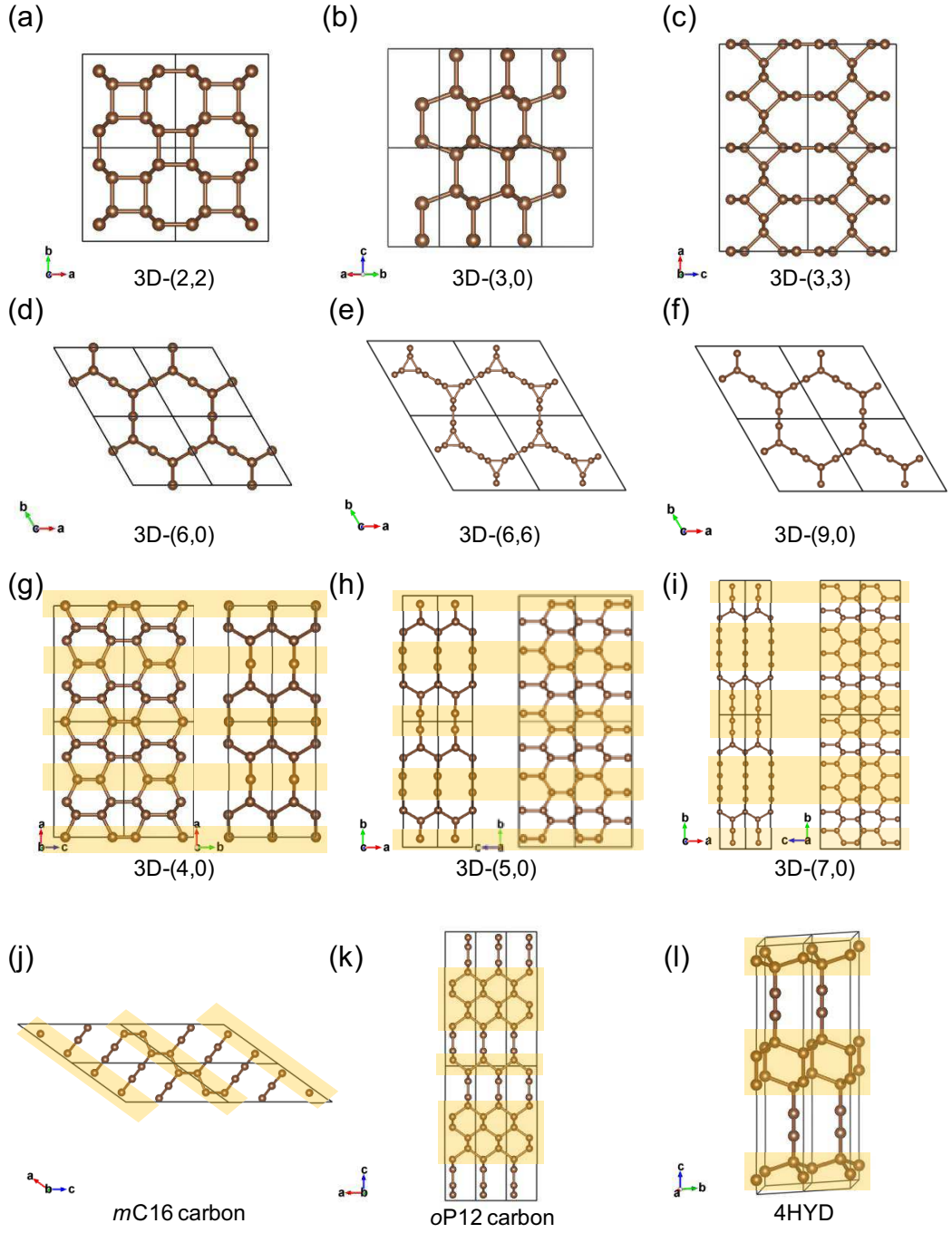


Fig. 2. Predicted crystal structures of superhard, low-density carbon polymers. (a–i) 3D carbon nanotubes polymers.[80] (j) and (k) 3D graphyne polymers.[83] (l) yne-diamond polymer.[82] The structure of 3D-(2,2) carbon (a) is the same as *bct*-C_4,[27] and (b) 3D-(3,0) carbon is actually the lonsdaleite structure. (a, b) sp^3 carbons; (c–k): sp^2-sp^3 carbons. (l) sp-sp^3 carbon. Due to the bonding difference, the carbon polymers possess distinct conductivity, such as insulating or semi-conducting characteristics with tunable band gaps (a–c) and novel (g) 1D, (h–i) 2D, and (d–f) 3D metallicities. The orange shadows represent insulating sp^3-hybridized carbon layers, which interrupt the electronic conduction in 3D.

Table 2. Space group (S.G.), density (g/cm^3), and calculated hardness (H, GPa), bulk modulus (B_0, GPa), B/G ratio, band gap (E_g, eV), axial tensile strength (σ_a, GPa), and radial tensile strength (σ_r, GPa) of various carbon polymers.

Structure	S.G.	Density	H	B	B/G	E_g	Hybridization	σ_a	σ_r	Refs.
3D-(3,0)	$P63/mmc$	3.62	96.9	454.5	0.82	3.05	sp^3	95.4	100.9	[80]
3D-(4,0)	$Immm$	3.31	56.8	372.8	1	semimetallic	sp^2+sp^3	142.3	69.4	
3D-(5,0)	$Cmcm$	3.2	40.9	352.5	1.23	metallic	sp^2+sp^3	160.2	50.5	
3D-(6,0)	$P6/mmm$	2.45	54.9	274.1	1.13	semimetallic	sp^2+sp^3	53.1	74.3	
3D-(7,0)	$Cmcm$	3.02	49.8	273.9	1.36	metallic	sp^2+sp^3	174.8	31.8	
3D-(8,0)	$Immm$	2.94	54.5	280.6	1.42	metallic	sp^2+sp^3	177.2	26.7	
3D-(9,0)	$P63/mmc$	1.9	36	207.7	2.05	metallic	sp^2+sp^3	119	51.5	
3D-(2,2)	$I4/mmm$	3.44	92.6	420.1	0.98	3.52	sp^3	112.4	93.8	
3D-(3,3)	$Cmmm$	3.05	90.9	343.9	1.21	1.21	sp^2+sp^3	130	76.5	
3D-(4,4)	$P4/mmm$	2.4	79.8	277.6	1.98	0.93	sp^2+sp^3	114.1	115.1	
3D-(6,6)	$P-62m$	1.72	46.7	195.4	2.07	semimetallic	sp^2+sp^3	83.1	50.8	
3D-(4,0)-I	$I4/mcm$	3.23	89.9	391.5	1.03	2.81	sp^2+sp^3	86	75	[79]
3D-(4,0)-II	$P4/mmm$	2.75	47.9	267.5	1.4	metallic	sp^2+sp^3	210	22.2	
3D-(4,0)-III	$Cccm$	3.35	91.9	398.7	0.96	3.09	sp^2+sp^3	89.8	97	
3D-(5,0)-I	$Cmmm$	2.66	83.2	283.1	1.38	0.29	sp^2+sp^3	127.1	38.3	
3D-(5,0)-II	$Pmma$	2.16	84.5	284.2	1.29	0.82	sp^2+sp^3	127.7	39.3	
3D-(5,0)-III	$Cmcm$	2.65	83.4	264.1	1.36	0	sp^2+sp^3	147.4	49	
3D-(6,0)-I	$P42/mmc$	2.59	81.07	298.6	1.29	0.69	sp^2+sp^3	112.2	70.5	
3D-(6,0)-II	$P42/mmc$	2.34	43	231.1	1.76	metallic	sp^2+sp^3	137.7	79.9	
3D-(6,0)-III	$P6/mcc$	2.91	83.7	334.1	0.95	2.29	sp^2+sp^3	77.8	72.6	
3D-(6,0)-IV	$Pccm$	2.71	80.1	212.6	0.83	0.23	sp^2+sp^3	34.5	60.7	
3D-(2,2)-I	$I4/mmm$	3.09	88.1	371.1	1.28	0.23	sp^2+sp^3	99.2	66.5	
3D-(2,2)-II	$I4/mmm$	2.99	93.6	415.6	0.96	3.45	sp^2+sp^3	96.3	112.9	
3D-(2,2)-III	$Cmmm$	3.51	95.2	427.7	0.88	2.97	sp^2+sp^3	113	93.4	
3D-(3,3)-I	$Cmmm$	3.05	90.9	343.9	1.21	1.24	sp^2+sp^3	130	76.6	
3D-(3,3)-II	$P63/mmc$	2.99	85.5	345.6	1.07	2.01	sp^2+sp^3	97.9	54.7	
3D-(3,3)-III	$P2/m$	3.11	85.3	356	1.03	2.88	sp^2+sp^3	99.9	69.1	
mC16	$C2/m$	3.14	41.6	347.5	1.2	metallic	sp^2+sp^3	/	/	[84]
oP12	$Pmma$	3.3	42.2	389.9	1.24	metallic	sp^2+sp^3	/	/	
2HYD	$P-6m2$	3.1	59.2	320.3	1.67	semimetallic	$sp+sp^3$	86.9	/	[82]
4HYD	$P62/mmc$	3.1	59.3	313.8	1.9	Semimetallic	$sp+sp^3$	88.5	/	

3.1.2. Boron nitrides

c-BN has thermal and chemical stabilities considered superior to those of diamond, although its crystal hardness is only half that of diamond. As such, the desirability to uncover novel B–N polymorphs to further increase hardness has not been stopped. Compressing BNNTs is expected to be one of the most promising approaches to obtain superhard B–N polymorphs. Similar to carbon nanotube polymers, a variety of 3D BNNT polymers, such as 3D-(n, 0) and 3D-(n, n) polymers, have been proposed.[85,86] Ultrahigh hardness, good ductility, high tensile strength, low density, and tunable band gaps make this class of B–N polymorphs of great interest in the viewpoints of scientific research and practical applications. As depicted in Fig. 3 and Table 3, the structures of 3D BNNT polymers highly depend on the size, geometry nanotube orientation, and the pressure and temperature conditions used.[86] At relatively low hydrostatic pressure, low-density 3D BNNT polymers can be produced by the direct linkage of their parent structures (Figs. 3(a)–3(c)). Meanwhile, at higher pressure, BNNTs would be further squeezed and deformed into dense 3D BNNT polymers forming sp^3-hybridized intratube B–N bonds, as seen from the 3D (4,4)-II structure (Fig. 3(e)). The calculated hardness values of the 3D BNNT polymers

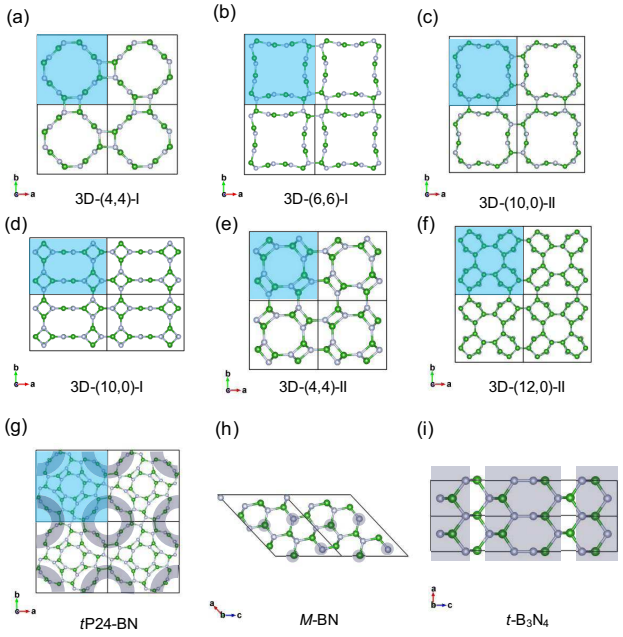


Fig. 3. Predicted crystal structures of boron nitrides. (a–g) 3D BNNT polymers.[85,86] The light blue shadows emphasize the components of parent BNNTs. For the 3D polymers in (a–c), they can be formed by compressing corresponding BNNTs at relative low pressures, and more dense forms of 3D polymers shown in (d–f) can be obtained at higher pressures. Distinct from the semiconducting 3D polymers in (a–f), the boron nitrides in (g–i) are conductive and considered rare.[85,87,89] The gray regions indicate the conductive units in structures, composed of sp^2 or sp^2/sp^3-hybridized bonding. The B and N atoms are painted in green and white colors, respectively. The hardness calculations indicate that these boron nitrides are all superhard except for *M*-BN (see detail in Table 3).

range from 55.1–66.6 GPa, demonstrating their potential application as superhard materials. According to the estimated Pugh's (B/G) ratios (Table 3), the 3D (4,4)-I, 3D (6,0)-I, and 3D (4,4)-V phases have better ductility than those of diamond. The band gaps also generally narrowed with the increase in sp^2/sp^3 ratios. For example, the structures of 3D (10,0)-I (Fig. 3(d)) and 3D (10,0)-II (Fig. 3(c)) contain 1/5 and 3/5 sp^2/sp^3 fractions, respectively, leading to the corresponding band gaps of 3.92 and 2.56 eV. In particular, the full sp^3-hybridized 3D (10,0)-III was predicted to be a semiconductor with a direct band gap.

Another new sp^2-sp^3 BN structure, *M*-BN, (Fig. 3(h)) was proposed based on the CALYPSO algorithm.[87] Its structure comprises puckered h-BN layers interlinked by partial sp^3 B–N bonds. Taking its 1D metallicity into account, its calculated hardness is 33.7 GPa lower than that of *c*-BN.[88] In addition, a tetragonal B_3N_4 (*t*-B_3N_4, Fig. 3(i)) containing sp^3*c*-BN blocks and sp^2 N–N bonds possessing high hardness value of 42.5 GPa was reported and identified as the hardest B_3N_4 polymorph predicted so far.[89] Compared with other proposed B_3N_4 polymorphs,[90] the strong N–N bonds in *t*-B_3N_4 along the *c* axis lead to axial ultra-incompressibility, and the insulating boron sheets stacked along the *c* axis interrupt the conduction, resulting in 2D metallicity. In addition, *t*-B_3N_4 possesses the combined mechanical and electrical properties of superhardness, ultra-incompressibility, and 2D metallicity in a 3D framework.

Table 3. Space group (S.G.), density (g/cm^3), and calculated hardness (H, GPa), bulk modulus (B_0, GPa), B/G ratio, band gap (E_g, eV), sp^2/sp^3 atomic ratio, axial tensile strength (σ_a, GPa) and radial tensile strength (σ_r, GPa) of various boron nitrides.

Structure	S.G.	Density	H	B	B/G	E_g	Hybridization	σ_a	σ_r	Refs.
cBN	F-43m	3.46	65.5	366.5	0.95	insulating	sp^3	/	/	
3D-(6,0)-I	P42mc	2.56	56.1	258.4	1.65	3.21	sp^2+sp^3	60.7	52	[86]
3D-(6,0)-II	Abm2	3.34	63.4	342	1.09	4.57	sp^3	67.5	49.1	
3D-(8,0)-I	I4cm	3.19	60.6	333.9	1.18	4.52	sp^3	64.9	56.8	
3D-(8,0)-II	Iba2	3.39	64.3	350.4	1.02	4.61	sp^3	68.5	72.3	
3D-(10,0)-I	Abm2	2.92	58.8	297.4	1.39	3.92	sp^2+sp^3	64.9	41.6	
3D-(10,0)-II	P42cm	2.32	55.1	134.5	1.21	2.56	sp^2+sp^3	60.5	34.8	
3D-(10,0)-III	Pcc2	3.27	62.4	332.5	1.09	4.7	sp^3	66.4	58.1	
3D-(12,0)-I	Abm2	2.77	58.1	273.2	1.51	3.78	sp^2+sp^3	64.8	32.9	
3D-(12,0)-II	I4cm	3.06	62.2	245.5	1.12	3.81	sp^2+sp^3	71.2	43.5	
3D-(12,0)-III	Iba2	3.45	65	361.6	1	4.71	sp^3	69.3	73.1	
3D-(4,4)-I	$P$4/mbm	2.37	55.3	234.3	2.06	3.45	8/8	77.3	39.8	
3D-(4,4)-II	$I$4/m	3.04	60	299.7	1.44	3.34	sp^3	74.5	49.7	
3D-(4,4)-III	$P$42/mnm	3.4	64.9	358.6	1.12	4.67	sp^3	85.1	70	
3D-(4,4)-IV	$Pbam$	3.48	65.8	368.1	1.02	5.09	sp^3	86.3	69.9	
3D-(4,4)-V	$Cmmm$	2.85	62.4	256.4	1.62	3.21	sp^2+sp^3	88.5	39.9	
3D-(6,6)-I	$P$42/m	2.61	57	236.7	1.46	2.92	sp^2+sp^3	80.4	34.9	
3D-(6,6)-II	$P$2/m	3.45	65.5	363.9	1.05	4.97	sp^3	86	69.7	
3D-(6,6)-III	$Pnnm$	3.5	66.6	373.4	1	5.01	sp^3	86.6	70.2	
3D-(6,6)-IV	$Immm$	3.01	62.9	291.9	1.48	3.75	sp^2+sp^3	92.7	57.3	
3D-(6,6)-V	$P$2/m	2.78	59.9	257.4	1.53	3.48	sp^2+sp^3	77.3	30.5	
3D-(6,6)-VI	$C$2/m	3.4	63.9	341.1	1.08	5.56	sp^3	84.8	46	
3D-(8,8)-I	$P$2/m	3.48	66.1	368.7	1.02	4.92	sp^3	86.3	70	
M-BN	Cm	3.33	33.7	/	/	metallic	sp^2+sp^3	/	/	[87]
t-B_3N_4	I-4m2	3.34	42.5	311.7	1.28	metallic	4/10	/	/	[89]
*t*P24-BN	$P4/m$	2.94	37.8	220.9	1.17	metallic	sp^2+sp^3	/	/	[85]
*m*P28-BN	$P2/m$	3.45	63.2	360.9	1.04	1.28	sp^3	/	/	
*o*P26-BN	Pmc21	3.11	61.5	310.6	1.24	2.15	sp^2+sp^3	/	/	
*t*P28-BN	P42cm	3.08	45.6	288.1	1.24	3.13	sp^2+sp^3	/	/	

3.1.3. B–C–N compounds

Diamond and *c*-BN are two classes of excellent superhard materials, thus, ternary B–C–N compounds are expected to be the best candidates for superhard materials. Many experimental and theoretical studies have focused on BC_xN compounds. Particularly, the diamond-like *c*-BC_2N, regarded as the ideal mixture of diamond and *c*-BN, has been investigated extensively and reported to have a high Vickers hardness (76 GPa).[10,13] BC_2N structures are predicted to be superhard through hardness calculations.[13,91–94] In addition, it has been reported that greater C–C bonding in BC_xN is beneficial to the enhancement of hardness. Thus, diamond-like BC_6N attracted considerable attention from researchers. Two high-density hypothetical BC_6N structures, i.e., *t*-BC_6N and *r*-BC_6N (Figs. 4(a) and 4(b)), have been predicted to be superhard with hardness value of approximately 80 GPa.[12] However, the commonly proposed BC_xN are classifies as semiconductors or insulators due to their similar isoelectronic properties with diamond. Therefore, the design of superhard and metallic BC_xN was anticipated by researchers. Based on

first-principle calculations, several superhard BC_xN structures (Fig. 4(c) and 4(d)) have been designed by replacing partial B and N atoms in the o-B_3N_5 structure,[95] and the resulting sandwich-structured o-BC_6N, t-BC_6N-1, t-BC_6N-2, and o-BC_2N exhibit intriguing electrical properties, including 1D and/or 2D metallicity due to the presence of sp^2-hybridized atoms.[11,12,14]

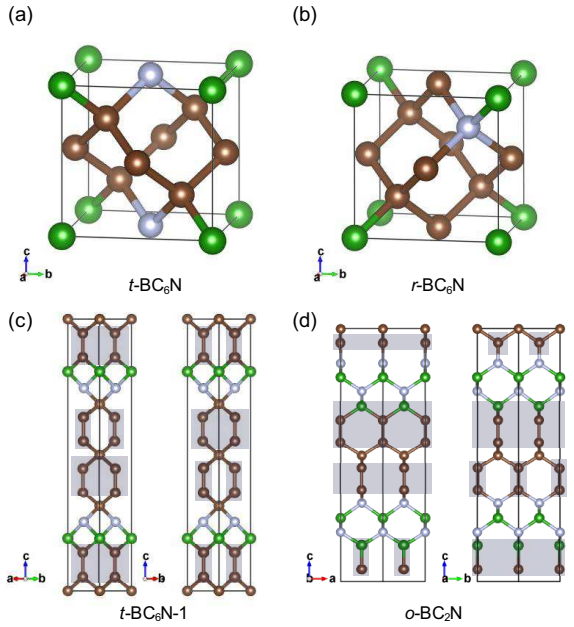


Fig. 4. Predicted crystal structures of superhard B–C–N compounds. (a) and (b) are the structures of sp^3 BC_6N that originated from diamond structure,[12] and (c) and (d) are low-density sp^2-sp^3 BC_2N structures that originated from $C222_1$-B_3N_5.[11,14] (c) t-BC_6N-1 possesses novel 1D metallicity, and (d) o-BC_2N possesses both 1D and 2D metallicities. The gray shadows represent the conductive units. The C, B, and N atoms are painted in brown, green, and white colors, respectively.

3.1.4. Carbon nitrides

Since the first prediction of low-compressibility C_3N_4 in 1996,[96] the search for carbon nitrides with hardness that is higher than diamond has become the holy grail in the field of superhard materials. Considerable experimental and theoretical studies have attempted to search for such high-hardness compounds. In early predictions, a number of hypothetical C_3N_4 structures were proposed by atomic substitution based on the known A_3B_4 structural types,[97–99] but their existence was still ambiguous because of the limited quantity and heterogeneity of the synthesized samples in experiments.[93] Although the C_3N_4 polymorphs have a very high predicted bulk moduli exceeding that of diamond, the most stable composition of C–N compounds is still inconclusive.[97,101] Therefore, several attempts were made to explore carbon nitrides with different stoichiometric ratios.

One prior theoretical study proposed a diamond-like $C_{11}N_4$ (d-CN) through the possible phase transition of graphite-like $C_{11}N_4$ (g-CN) under pressure.[102] As shown in Fig. 5(b), d-cn involves polyhedral hollow C–N cages with a theoretical hardness value of 58 GPa and indirect band gap of 1.86 eV. A body-centered tetragonal bct-CN_2 (Fig. 5(c)) has also been predicted at high pressure based on CALYPSO search.[103] Its structure contains strong covalent C–N and N–N bonds, which leads to its high bulk (407 GPa) and shear (386 GPa) moduli as well as estimated hardness (77 GPa). However, the flexibility and mobility of the non-bonding lone-pair states in structure also leads to a relatively low ideal shear strength of 47 GPa. For 1:1 CN compounds, a sp^2-sp^3 *Pnnm* CN (Fig. 5(d)) with hardness of 62.3 GPa has been proposed theoretically.[104] Subsequently, the experimental synthesis of a β-InS-type CN phase, which is identical to the theoretically predicted *Pnnm* CN, has been reported to be synthesized at high pressure and temperature conditions implemented in the diamond anvil cell (DAC).[105] This study indicates that *Pnnm* CN is semiconducting with a wide band gap of 3.7 eV and agrees well with the experimental observation of the transparency of sample during laser heating. This work pointed out new directions in the search for superhard carbon nitride materials with different stoichiometric ratios for future technological applications.

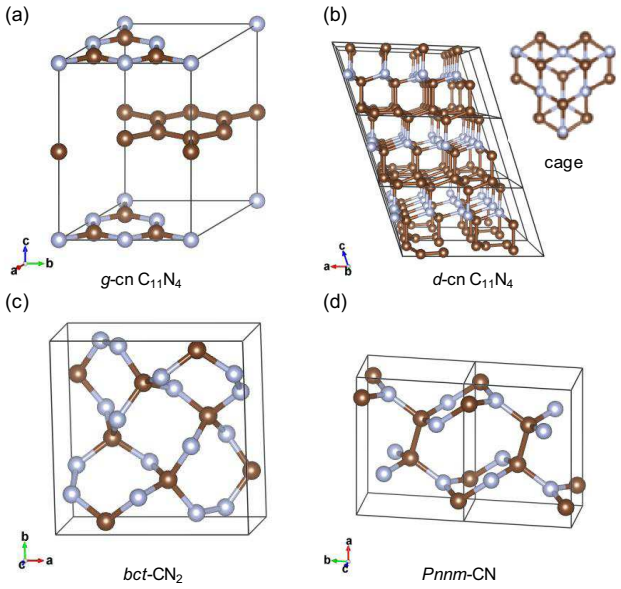


Fig. 5. Predicted crystal structures of carbon nitrides. The compression of graphite-like $C_{11}N_4$ (a) can obtain the superhard diamond-like $C_{11}N_4$ (b), and the inset in (b) represents a cage-like part structure.[138] (c) Superhard sp^2-sp^3 CN_2 with body-centered tetragonal structure and calculated hardness of 77.4 GPa.[103] (d) β-InS-type CN structure recently synthesized at HPHT with calculated hardness of 62.3 GPa.[105,139] The C and N atoms are painted in brown and white colors, respectively.

3.1.5. Boron carbides

For decades, many experimental and theoretical efforts have been made to study boron carbides, typically B_4C[8] and $B_{13}C_2$,[19] due to their high hardness and strength at high temperature. In addition, d-BC_x possesses higher stability and antioxidant ability compared with diamond as well as peculiar metallicity and superconductivity. The unique combination of mechanical, electronic, and thermal properties has promoted the studies of electric devices under extreme conditions. The

high superconductive transition temperature (T_c) is expected to be obtained by the heavy boron doping in diamond. Unfortunately, it was difficult to achieve d-BC_x when the doped B content exceeded approximately 5% in experiments. Nevertheless, d-BC_x ($x = 2.8 \pm 0.7$ or 5) has been synthesized from high pressure and temperature experiments by directly compressing graphite-like BC_x (g-BC_x).[8,9,52] In view of the small nanocrystalline size in microstructure, the composition and atomic positions in d-BC_x cannot be easily determined by common experimental methods.

Theoretically, a series of candidate d-BC_x ($x = 2$, 3, 5, 7) structures have been proposed.[53–55,106–112] Comparing experimental and theoretical data (e.g., XRD and Raman spectra), some reasonable structures can explain the experimental observations. For instance, an orthorhombic *Pmma*-b BC_3[108] (Fig. 6(b)) has been considered as a good candidate structure for synthesized d-BC_3 in previous reports,[52] and subsequent studies illuminated that monoclinic M-BC_3 (Fig. 6(c)) may also be the coexistent phase.[109] Another cubic I-43m BC_3 (Fig. 6(d)) structure has been proposed to match the experimentally reported c-BC_3.[9,107] In addition, several d-BC_5 (Figs. 6(e)–6(h)) structures have been proposed to account for the superhard BC_5 synthesized in experiments.[55] Considering that the composition of synthetic d-BC_x have been determined by energy dispersive X-ray spectrum (EDS) with large error, studies of d-BC_x with other chemical compositions are also necessary. Potential BC_7 (Figs. 6(i)–6(l)) structures have been uncovered by performing variable-cell structure simulations.[111,112] The estimated hardness of these low-energy BC_7 structures are approximately 80 GPa, indicating their superhard nature. As depicted in Table 4, the proposed BC_x structures exhibit metallicity and are considered as potential superhard materials. The conductivity may have originated from the introduction of B atoms lacking an electron compared with C atoms, especially because no obvious dependence has been observed between T_c and B concentration. However, hardness significantly increased with increased C content due to the increased fraction of covalent C–C bonds.

Table 4. Space group (S.G.), and calculated bulk modulus (B_0, GPa), hardness (H, GPa), and superconducting transition temperature (T_c, K) of predicted BC_x structures.

Structure	S. G.	B_0	H	T_c	Refs.
t-BC_2	$I4_1/amd$	349	56	/	[106]
BC_3	P-4m2	359.1	65.8	13.4–19.5	[108]
BC_3	*Pmma*-a	354.2	61.9	16.6–23.4	
BC_3	*Pmma*-b	351.8	64.8	4.9–8.8	
M-BC_3	$C2/m$	/	43.8	/	[109]
d-BC_3	I-43m	/	62	/	[107]
BC_5	$P3m1$	381	64	41.5–47.0	[55]
BC_5	P-3m1-1	379	63	33.6–38.8	
BC_5	P-3m1-2	398	61	/	
BC_5	$Imm2$	376	65	23.1–28.3	
BC_5	I-4m2	381	71	8.5–11.8	
BC_5	*Pmma*-1	373	74	8.4–11.3	
BC_5	*Pmma*-2	379	70	18.1–22.6	
BC_7	P-4m2	377	75.2	/	[111]
BC_7	$P3m1$	378	65.3	/	
BC_7	$Pmm2$	377	80.7	/	
BC_7	$R3m$	378	65.4	/	
BC_7	P-43m	375	77.6	/	
BC_7	P-4m2	388	78	8.4–11.4	[112]

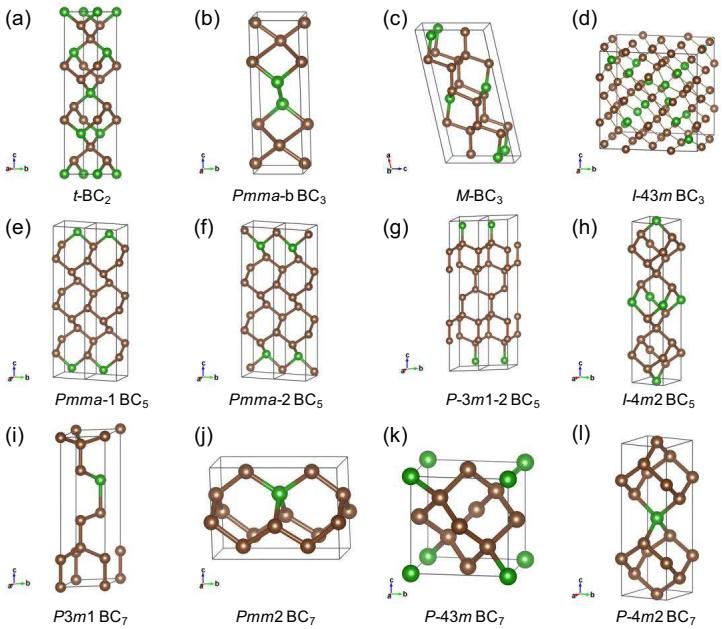


Fig. 6. Predicted crystal structures of superhard diamond-like boron carbides. (a) Tetragonal BC_2.[106] (b–d) BC_3, (e–h) BC_5, and (i–l) BC_7 structures, respectively.[54,100–102,104,105] The BC_3 and BC_5 structures have been suggested as reasonable solutions for the experimentally synthesized superhard boron carbide phases.[7,9,52] As seen from Table 4, these structures have high theoretical hardness values, which are above 40 GPa, and are commonly metallic due to the addition or doping of boron. Notably, the structures in (b), (e), (f), (h), and (i) are also superconductive. There is no obvious dependence between T_c and the concentration of B; however, hardness has significantly increased with increased C content. C and B atoms are painted in brown and green colors, respectively.

3.1.6. B–N/C–O compounds

As a result of the reported synthesis of B_2O,[113] the ternary compounds in the B–C/N–O system are considered as candidate superhard materials. Using crystal structure prediction, the structures of B_2CO were explored in past studies.[20,21] Three hypothetical structures (Figs. 7(a)–7(c)), tI16-B_2CO, tP4-B_2CO, and oP8-B_2CO, were assembled by sp^3 B–C and B–O bonds. Compared with diamond-like B_2O, the lengths of B–O bonds are similar, but the B–C bonds are much shorter in B_2CO. As a result, B_2CO, with a calculated Vickers hardness of 50 GPa, is harder than B_2O (38 GPa).[18,20,21] B_3NO, like B_2CO, is isoelectronic with diamond. A search for superhard materials based on CALYPSO method has been used to explore new B_3NO structures. As shown in Figs. 7(s)–7(f), two orthorhombic structures, oI20-B_3NO and oP20-B_3NO, with calculated Vickers hardness values of 45.9 and 47.4 GPa, respectively, have been proposed.[23] The present results reveal that B_3NO structures can stabilize in a 3D network with typically strong covalent B–B, B–N, and B–O bonds. The B–N bonds in B_3NO are shorter than those in B_2O, resulting in higher hardness. A high calculated elastic modulus indicates that these structures are highly incompressible.

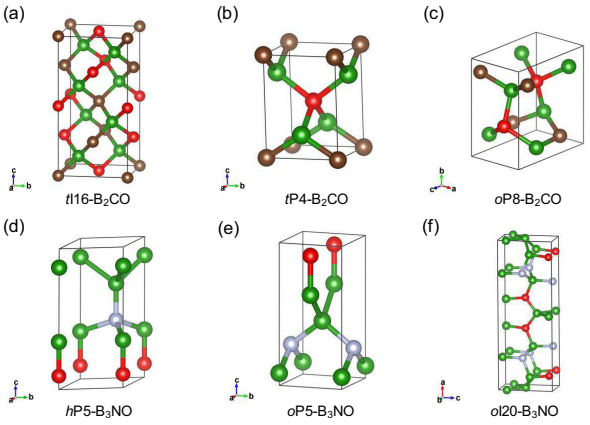


Fig. 7. Predicted crystal structures of superhard B–C/N–O compounds. (a–c) Hypothetical diamond-like B_2CO structures with covalent sp^3 B–C and B–O bonds.[20,21] (d–f) Hypothetical B_3NO structures with covalent B–B, B–N, and B–O bonds.[23] All structures are isoelectronic with diamond, indicating their semiconducting characteristics. Their hardness value is approximately 50 GPa. The B, C, N, and O atoms are painted in green, brown, white, and red colors, respectively.

3.1.7. Si–C–N compounds

The binary compounds of silicon carbide (SiC) and silicon nitride (Si_3N_4) have received much research attention in the past due to their wide applications as structural materials. Their composites have also been studied for a long time.[114] However, the synthesis of hard or superhard Si–C–N compounds has yet to be achieved.[115] Structure prediction was performed by first-principle calculations,[116] and three low-energy SiCN were reported (Fig. 8). t-SiCN (Fig. 8(a)) is a superhard semiconductor with a narrow band gap of 0.89 eV and hardness of 41.5 GPa. In addition, the long bonds in Si–C–N compounds tend to limit their hardness. Through a comparison of their thermodynamic stability, h-SiCN (Fig. 8(b)) and o-SiCN (Fig. 8(c)) may be considered as possible high-pressure phases of t-SiCN, and their phase transitions may occur at 21.6 and 21.9 GPa, respectively.

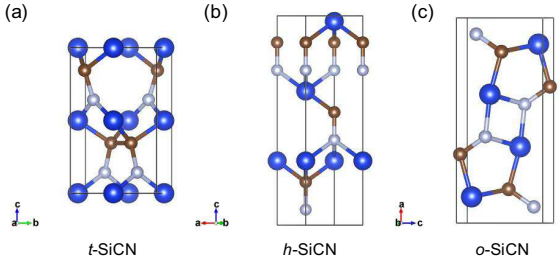


Fig. 8. Predicted crystal structures of SiCN compounds. The calculation of total enthalpy with pressure indicates that (a) t-SiCN may change into (b) h-SiCN and (c) o-SiCN under high pressures of 21.9 and 21.6 GPa, respectively.[116] (a) t-SiCN was a narrow gap semiconductor with a band gap of 0.89 eV, and (b) h-SiCN and (c) o-SiCN are metallic. The calculated hardness of (a) t-SiCN is 41.5 GPa. The Si, C, and N atoms are painted in blue, brown and white colors, respectively.

3.2. Transition-metal light-element compounds

TM-LE compounds, such as transition-metal borides (TMBs), carbides (TMCs), and nitrides (TMNs), have outstanding mechanical properties and have been considered as promising candidates for superhard materials. However, because of the large differences in atomic number and mass between TMs and LEs, their structures are difficult to determine in experiments and are often controversial.[117] Consequently, studies of TM-LE compounds have been intensified for decades. On many prior attempts, a variety of TM-LE compounds have been studied, for example, Fe_2B, FeB_4, RhB, WB_x, Na_2B_{30}, RuC, Re_2 C, Zr_3N_4, PtN_2, and IrN_2.[36,37,56,117–126] The synthesized oP10-FeB_4 (Fig. 9(a)) was initially considered as a candidate superhard material with hardness exceeding 40 GPa,[125,127] but later studies suggested that it was unlikely to be superhard because of the weak Fe–B bonding and because the measured hardness of polycrystalline FeB_4 bulk material was only 10–30 GPa.[128–130] Using structure prediction, a new form of FeB_4, tP10-FeB_4 (Fig. 9(b)), was proposed and was obtained by compressing oP10-FeB_4 above 65.9 GPa.[122] It is semiconducting, which is rare in metal borides, and enhances the electron locations, resulting in an estimated hardness value of as high as 45 GPa. For WB_x compounds, structure predictions were carried out in a wide range of chemical compositions.[35,131–134] The synthesized γ-W_2B, α-WB, and ε-WB_2, were well matched with the predicted structures of $I4/m$-4u, $I41/amd$-8u, and $P63/mmc$-4u, respectively.[131,132] The structural identification of syntheyized WB_4 has generated great interest and controversy. Initially, it was assumed to be in a hexagonal $P63/mmc$-4u WB_4,[135] and subsequent analysis of thermodynamic and

lattice stabilities suggested that it should be described as $P63/mmc$-4u WB_3.[112,115] Further calculations of stress-strain relations demonstrated that the rising boron concentrations in WB_x ($x = 1, 2, 3, 4$) result in little improvement or even trend downward with rising boron content in most cases, for example, the indentation stress peaks under (1-10)[110]-orientation largely decrease going from WB_2 ($\sim$ 50 GPa) to WB_3 ($\sim$ 30 GPa), and then recover for WB_4 ($\sim$ 35 GPa).[131] In addition, the high-pressure phase transitions of $B1$-structured stoichiometric TMCs (TM=Ti, Zr, Hf, V, Nb, and Ta) were investigated using *ab initio* calculations.[137] The study found two intriguing phase-transition routes and a high-pressure phase of T1I'-type, namely, $B1 \rightarrow$ distorted T1I (T1I')$\rightarrow$ TT1I and /or $B1 \rightarrow$ and/or TiB (TiB')$\rightarrow$ BTiB. This suggests that TiB-type phase is a high-pressure phase and T1I'-type phase may be recovered at ambient pressure. These findings provide crucial insights for understanding the rich and complex crystal structures of TM-LE compounds, which have broad implications for further exploration.

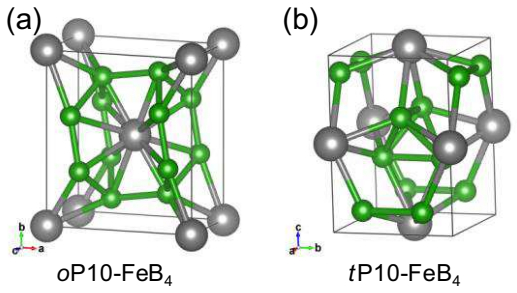


Fig. 9. Crystal structures of FeB_4. (a) oP10-FeB_4 with an orthorhombic structure, which was first predicted by Kolmogorov *et al.*,[127] and was later successfully synthesized at HPHT conditions.[125] This type of FeB_4 is a superconductor with measured T_c below 2.9 K; its hardness was first measured to be 62 GPa[125] and later proven to be $\sim$ 10–30 GPa.[128–130] (b) tP10-FeB_4 as a predicted high-pressure phase. This phase is a superhard semiconductor with band gap of approximately 1.85 eV and calculated hardness of 45 GPa.[122] The B and Fe atoms are painted in gray and green colors, respectively.

4. Conclusion and perspectives

Exploring superhard materials is an important topic due to their scientific interest and potential application. Here, we present a short review of recent advances in the discovery of superhard materials in LE compounds and TM-LE compounds using advanced CALYPSO structure prediction. A large number of promising, predicted crystal structures have excellent properties, including ultrahigh hardness, semiconductivity, and superconductivity, and some of them are very helpful in understanding the phases that cannot be completely determined experimentally. Nevertheless, current methodologies are mainly effective for structure predictions of single-crystal materials. The properties of polycrystalline materials, including hardness, are dependent not only on intrinsic crystal structures, but also on their microstructures such as defects, dislocation, grain size, and boundary. The investigations have proven that nanostructuring or nanotwinning can significantly enhance the hardness of polycrystalline covalent materials. For example, the synthesized nanotwinned diamond exhibits extremely high hardness, which is twice that of a single crystal of diamond.[1,2] Therefore, developing a general approach of structure prediction for both single-crystal and polycrystalline materials is highly anticipated, and this will lead to new directions in searching for superhard materials among promising polycrystalline systems.

References

[1] Huang Q, Yu D, Xu B, Hu W, Ma Y, Wang Y, Zhao Z, Wen B, He J, Liu Z and Tian Y 2014 *Nature* **510** 250
[2] Tian Y, Xu B, Yu D, Ma Y, Wang Y, Jiang Y, Hu W, Tang C, Gao Y, Luo K, Zhao Z, Wang L M, Wen B, He J and Liu Z 2013 *Nature* **493** 385
[3] Zhao Z, Xu B and Tian Y 2016 *Annu. Rev. Mater. Res.* **46** 383
[4] Zhu C, Bi H, Zhang S, Wei S and Li Q 2015 *RSC Adv.* **5** 65745
[5] Zhu C, Li Q, Zhou Y, Zhang M, Zhang S and Li Q 2014 *J. Phys. Chem. C* **118** 27252
[6] Hu Y J , Xu S L , Wang H, Liu H, Xu X C and Cai Y X 2016 *Chin. Phys. Lett.* **33** 106102
[7] Calandra M and Mauri F 2008 *Phys. Rev. Lett.* **101** 016401
[8] Solozhenko V L, Kurakevych O O, Andrault D, Le Godec Y and Mezouar M 2009 *Phys. Rev. Lett.* **102** 015506
[9] Zinin P V, Ming L C, Ishii H A, Jia R, Acosta T, Hellebr and E 2012 *J. Appl. Phys.* **111** 114905
[10] Solozhenko V L, Andrault D, Fiquet G, Mezouar M and Rubie D C 2001 *Appl. Phys. Lett.* **78** 1385
[11] Gao Y, Wu Y, Huang Q, Ma M, Pan Y, Xiong M, Li Z, Zhao Z, He J and Yu D 2018 *Comput. Mater. Sci.* **148** 157
[12] Luo X, Guo X, Liu Z, He J, Yu D, Tian Y and Wang H T 2007 *J. Appl. Phys.* **101** 083505
[13] Sun H, Jhi S H , Roundy D, Cohen M L and Louie S G 2001 *Phys. Rev. B* **64** 094108
[14] Gao Y, Wu Y, Huang Q, Ma M, Pan Y, Xiong M, Li Z, Zhao Z, He J and Yu D 2017 *J. Appl. Phys.* **121** 225103
[15] Oganov A R, Chen J, Gatti C, Ma Y, Ma Y, Glass C W, Liu Z, Yu T, Kurakevych O O and Solozhenko V L 2009 *Nature* **457** 863
[16] An Q, Reddy K M, Xie K Y, Hemker K J and Goddard W A 2016 *Phys. Rev. Lett.* **117** 085501
[17] He X L , Shao X, Chen T, Tai Y K , Weng X J , Chen Q, Dong X, Gao G, Sun J, Zhou X F , Tian Y and Wang H T 2019 *Phys. Rev. B* **99** 184111
[18] He D, Zhao Y, Daemen L, Qian J, Shen T D and Zerda T W 2002 *Appl. Phys. Lett.* **81** 643
[19] Guo X, He J, Liu Z, Tian Y, Sun J and Wang H T 2006 *Phys. Rev. B* **73** 104115
[20] Li Y W, Li Q and Ma Y M 2011 *EPL Europhys. Lett.* **95** 66006
[21] Liu C, Zhao Z, Luo K, Hu M, Ma M and He J 2017 *Diam. Relat. Mater.* **73** 87
[22] Zhang M, Yan H, Zheng B and Wei Q 2015 *Sci. Rep.* **5** 15481
[23] Li Q, Wang J, Zhang M, Li Q and Ma Y 2015 *RSC Adv.* **5** 35882
[24] Hu M, He J, Zhao Z, Strobel T A, Hu W, Yu D, Sun H, Liu L, Li Z, Ma M, Kono Y, Shu J, Mao H, Fei Y, Shen G, Wang Y, Juhl S J, Huang J Y, Liu Z, Xu B and Tian Y 2017 *Sci. Adv.* **3** e1603213
[25] Wang Y, Panzik J E, Kiefer B and Lee K K M 2012 *Sci. Rep.* **2** 520
[26] Zhou X F , Qian G R , Dong X, Zhang L, Tian Y and Wang H T 2010 *Phys. Rev. B* **82** 134126
[27] Umemoto K, Wentzcovitch R M, Saito S and Miyake T 2010 *Phys. Rev. Lett.* **104** 125504
[28] Zhou R and Zeng X C 2012 *J. Am. Chem. Soc.* **134** 7530
[29] Tian F, Dong X, Zhao Z, He J and Wang H T 2012 *J. Phys. Condens. Matter* **24** 165504

[30] Zhao Z, Xu B, Zhou X F , Wang L M , Wen B, He J, Liu Z, Wang H T and Tian Y 2011 *Phys. Rev. Lett.* **107** 215502
[31] Zhao Y, He D W, Daemen L L, Shen T D, Schwarz R B, Zhu Y, Bish D L, Huang J, Zhang J, Shen G, Qian J and Zerda T W 2002 *J. Mater. Res.* **17** 3139
[32] Solozhenko V L 2002 *High Press. Res.* **22** 519
[33] Tian Y, Xu B and Zhao Z 2012 *Int. J. Refract. Met. Hard Mater.* **33** 93
[34] Li Q, Zhou D, Wang H, Chen W, Wu B, Wu Z and Zheng W 2012 *Solid State Commun.* **152** 71
[35] Gou H, Li Z, Wang L M , Lian J and Wang Y 2012 *AIP Adv.* **2** 012171
[36] Gao F, Xu R and Liu K 2005 *Phys. Rev. B* **71** 052103
[37] Yu R, Zhan Q and Zhang X F 2006 *Appl. Phys. Lett.* **88** 051913
[38] kirkpatrick S, Gelatt C D and Vecchi M P 1983 *Science* **220** 671
[39] Glass C W, Oganov A R and Hansen N 2006 *Comput. Phys. Commun.* **175** 713
[40] Deaven D M and Ho K M 1995 *Phys. Rev. Lett.* **75** 288
[41] Goedecker S 2004 *J. Chem. Phys.* **120** 9911
[42] Wales D J and Doye J P K 1997 *J. Phys. Chem. A* **101** 5111
[43] Pickard C J and Needs R J 2011 *J. Phys. Condens. Matter.* **23** 053201
[44] Wang Y, Lv J, Zhu L and Ma Y 2010 *Phys. Rev. B* **82** 094116
[45] Wang Y, Lv J, Zhu L and Ma Y 2012 *Comput. Phys. Commun.* **183** 2063
[46] Li Q, Ma Y, Oganov A R, Wang H, Wang H, Xu Y, Cui T, Mao H K and Zou G 2009 *Phys. Rev. Lett.* **102** 175506
[47] Amsler M, Flores-Livas J A, Lehtovaara L, Balima F, Ghasemi S A, Machon D, Pailhès S, Will, A, Caliste D, Botti S, San Miguel A, Goedecker S and Marques M A L 2012 *Phys. Rev. Lett.* **108** 065501
[48] Wang J T , Chen C and Kawazoe Y 2011 *Phys. Rev. Lett.* **106** 075501
[49] Wang J T , Chen C and Kawazoe Y 2012 *Phys. Rev. B* **85** 033410
[50] Mao W L 2003 *Science* **302** 425
[51] Wang Z, Zhao Y, Tait K, Liao X, Schiferl D, Zha C, Downs R T, Qian J, Zhu Y and Shen T 2004 *Proc. Natl. Acad. Sci.* **101** 13699
[52] Zinin P V, Ming L C, Kudryashov I, Konishi N and Sharma S K 2007 *J. Raman Spectrosc.* **38** 1362
[53] Yao Y, Tse J S and Klug D D 2009 *Phys. Rev. B* **80** 094106
[54] Jiang C, Lin Z and Zhao Y 2009 *Phys. Rev. B* **80** 184101
[55] Li Q, Wang H, Tian Y, Xia Y, Cui T, He J, Ma Y and Zou G 2010 *J. Appl. Phys.* **108** 023507
[56] Zhao Z, Cui L, Wang L M , Xu B, Liu Z, Yu D, He J, Zhou X F , Wang H T and Tian Y 2010 *Cryst. Growth* . **10** 5024
[57] Wang Y, Lv J, Li Q, Wang H and Ma Y 2019 *Handbook of Materials Modeling* (Cham: Springer International Publishing) pp. 1–28
[58] Su C, Lv J, Li Q, Wang H, Zhang L, Wang Y and Ma Y 2017 *J. Phys. Condens. Matter* **29** 165901
[59] Wang Y, Lv J, Zhu L, Lu S, Yin K, Li Q, Wang H, Zhang L and Ma Y 2015 *J. Phys. Condens. Matter* **27** 203203
[60] Wang Y and Ma Y 2014 *J. Chem. Phys.* **140** 040901
[61] Zhang X, Wang Y, Lv J, Zhu C, Li Q, Zhang M, Li Q and Ma Y 2013 *J. Chem. Phys.* **138** 114101
[62] Ceder G 2010 *MRS Bull.* **35** 693
[63] Lv J, Wang Y, Zhu L and Ma Y 2011 *Phys. Rev. Lett.* **106** 015503
[64] Wang H, Tse J S, Tanaka K, Iitaka T and Ma Y 2012 *Proc. Natl. Acad. Sci.* **109** 6463
[65] Li Y, Hao J, Liu H, Li Y and Ma Y 2014 *J. Chem. Phys.* **140** 174712
[66] Wang H, Wang Y, Lv J, Li Q, Zhang L and Ma Y 2016 *Comput. Mater. Sci.* **112** 406
[67] Li Q and Zheng W T 2016 *Chin. Phys. B* **25** 076103
[68] Zhao Z, Tian F, Dong X, Li Q, Wang Q, Wang H, Zhong X, Xu B, Yu D, He J, Wang H T , Ma Y and Tian Y 2012 *J. Am. Chem. Soc.* **134** 12362
[69] Zhu L, Liu H, Pickard C J, Zou G and Ma Y 2014 *Nat. Chem.* **6** 644
[70] Zhu L, Wang H, Wang Y, Lv J, Ma Y, Cui Q, Ma Y and Zou G 2011 *Phys. Rev. Lett.* **106** 145501
[71] Wang Y, Lv J, Zhu L and Ma Y 2010 *Phys. Rev. B* **82** 094116
[72] Zhang M, Liu H, Du Y, Zhang X, Wang Y and Li Q 2013 *Phys. Chem. Chem. Phys.* **15** 14120
[73] Li Z, Hu M, Ma M, Gao Y, Xu B, He J, Yu D, Tian Y and Zhao Z 2016 *Carbon* **105** 151
[74] Hu M, Tian F, Zhao Z, Huang Q, Xu B, Wang L M , Wang H T , Tian Y and He J 2012 *J. Phys. Chem. C* **116** 24233
[75] Somayazulu M, Ahart M, Mishra A K, Geballe Z M, Baldini M, Meng Y, Struzhkin V V and Hemley R J 2019 *Phys. Rev. Lett.* **122** 027001
[76] Drozdov A P, Kong P P, Minkov V S, Besedin S P, Kuzovnikov M A, Mozaffari S, Balicas L, Balakirev F F, Graf D E, Prakapenka V B, Greenberg E, Knyazev D A, Tkacz M and Eremets M I 2019 *Nature* **569** 528
[77] Zurek E 2019 *Physics* **12** 1
[78] Pan Y, Xie C, Xiong M, Ma M, Liu L, Li Z, Zhang S, Gao G, Zhao Z, Tian Y, Xu B and He J 2017 *Chem. Phys. Lett.* **689** 68
[79] Hu M, Zhao Z, Tian F, Oganov A R, Wang Q, Xiong M, Fan C, Wen B, He J, Yu D, Wang H T , Xu B and Tian Y 2013 *Sci. Rep.* **3** 1331
[80] Zhao Z, Xu B, Wang L M , Zhou X F , He J, Liu Z, Wang H T and Tian Y 2011 *ACS Nano* **5** 7226
[81] Pan Y, Hu M, Ma M, Li Z, Gao Y, Xiong M, Gao G, Zhao Z, Tian Y, Xu B and He J 2017 *Carbon* **115** 584
[82] Hu M, Huang Q, Zhao Z, Xu B, Yu D and He J 2014 *Diam. Relat. Mater.* **46** 15
[83] Hu M, He J, Wang Q, Huang Q, Yu D, Tian Y and Xu B 2014 *J. Superhard Mater.* **36** 257
[84] Hu M, Pan Y, Luo K, He J, Yu D and Xu B 2015 *Carbon* **91** 518
[85] Xiong M, Luo K, Yu D, Zhao Z, He J and Gao G 2017 *J. Appl. Phys.* **121** 165106
[86] Xiong M, Fan C, Zhao Z, Wang Q, He J, Yu D, Liu Z, Xu B and Tian Y 2014 *J. Mater. Chem. C* **2** 7022
[87] Xiong M, Luo K, Pan Y, Liu L, Gao G, Yu D, He J, Xu B and Zhao Z 2018 *J. Alloys Compd.* **731** 364
[88] Guo X, Li L, Liu Z, Yu D, He J, Liu R, Xu B, Tian Y and Wang H T 2008 *J. Appl. Phys.* **104** 023503
[89] Xie C, Ma M, Liu C, Pan Y, Xiong M, He J, Gao G, Yu D, Xu B, Tian Y and Zhao Z 2017 *J. Mater. Chem. C* **5** 5897
[90] Zhang B 2016 *J. Alloys Compd.* **663** 862
[91] Mattesini M and Matar S F 2001 *Int. J. Inorg. Mater.* **3** 943
[92] Tateyama Y, Ogitsu T, Kusakabe K, Tsuneyuki S and Itoh S 1997 *Phys. Rev. B* **55** R10161
[93] Zhou X F , Sun J, Qian Q R , Guo X, Liu Z, Tian Y and Wang H T 2009 *J. Appl. Phys.* **105** 093521
[94] Zhou X F , Sun J, Fan Y X , Chen J, Wang H T , Guo X, He J and Tian Y 2007 *Phys. Rev. B* **76** 100101
[95] Li Y, Hao J, Liu H, Lu S and Tse J S 2015 *Phys. Rev. Lett.* **115** 105502
[96] Teter D M and Hemley R J 1996 *Science* **271** 53
[97] Liu A Y and Cohen M L 1990 *Phys. Rev. B* **41** 10727
[98] Guo Q, Xie Y, Wang X, Lv S, Hou T and Liu X 2003 *Chem. Phys. Lett.* **380** 84
[99] Zinin P V, Ming L C, Sharma S K, Hong S M, Xie Y, Irifune T and Shinmei T 2008 *J. Phys. Conf. Ser.* **121** 062002
[100] Liu J, Sekine T and Kobayashi T 2006 *Solid State Commun.* **137** 21
[101] Liu A Y and Cohen M L 1989 *Science* **245** 841
[102] Li D, Shi J, Lai M, Li R and Yu D 2014 *Phys. B Condens. Matter* **449** 90
[103] Li Q, Liu H, Zhou D, Zheng W, Wu Z and Ma Y 2012 *Phys. Chem. Chem. Phys.* **14** 13081
[104] Zhang M, Wei Q, Yan H, Zhao Y and Wang H 2014 *J. Phys. Chem. C* **118** 3202
[105] Stavrou E, Lobanov S, Dong H, Oganov A R, Prakapenka V B, Konôpková Z and Goncharov A F 2016 *Chem. Mater.* **28** 6925
[106] Xu L, Zhao Z, Wang L M , Xu B, He J, Liu Z and Tian Y 2010 *J. Phys. Chem. C* **114** 22688
[107] Zhang M, Liu H, Li Q, Gao B, Wang Y, Li H, Chen C and Ma Y 2015 *Phys. Rev. Lett.* **114** 015502
[108] Liu H, Li Q, Zhu L and Ma Y 2011 *Phys. Lett. A* **375** 771
[109] Ma M, Yang B, Hu M, Li Z, Wang Q, Cui L, Yu D and He J 2015 *Phys. Chem. Chem. Phys.* **17** 9748
[110] Liu Z, He J, Yang J, Guo X, Sun H, Wang H T , Wu E and Tian Y 2006 *Phys. Rev. B* **73** 172101
[111] Liu H, Li Q, Zhu L and Ma Y 2011 *Solid State Commun.* **151** 716
[112] Xu L, Zhao Z, Wang Q, Wang L M , Xu B, He J and Tian Y 2011 *J. Appl. Phys.* **110** 013501
[113] Li Q, Chen W, Xia Y, Liu Y, Wang H, Wang H and Ma Y 2011 *Diam. Relat. Mater.* **20** 501
[114] Riedel R, Greiner A, Miehe G, Dressler W, Fuess H, Bill J and Aldinger F 1997 *Angew. Chem. Int. Ed. Engl.* **36** 603
[115] Chen L C, Chen K H, Wei S L, Kichambare P D, Wu J J, Lu T R and Kuo C T 1999 *Thin Solid Films* **355–356** 112

[116] Cui L, Wang Q, Xu B, Yu D, Liu Z, Tian Y and He J 2013 *J. Phys. Chem. C* **117** 21943

[117] Zhao Z, Xu L, Wang L M , Xu B, Wang M, Liu Z and He J 2011 *Comput. Mater. Sci.* **50** 1592

[118] Deng S, Zhao J, Wei S, Zhu C, Lv J, Li Q and Zheng W 2016 *RSC Adv.* **6** 73576

[119] Zhao Z, Wang M, Cui L, He J, Yu D and Tian Y 2010 *J. Phys. Chem. C* **114** 9961

[120] Zhao Z, Xu L, Wang M, Cui L, Wang L M , He J, Liu Z and Tian Y 2010 *Phys. Status Solidi RRL - Rapid Res. Lett.* **4** 230

[121] Zerr A, Miehe G and Riedel R 2003 *Nat. Mater.* **2** 185

[122] Wang Q, Zhang Q, Hu M, Ma M, Xu B and Tian Y 2014 *Phys. Chem. Chem. Phys.* **16** 22008

[123] Wang Q, Zhao Z, Xu L, Wang L M , Yu D, Tian Y and He J 2011 *J. Phys. Chem. C* **115** 19910

[124] Wang Y X, Arai M, Sasaki T and Fan C Z 2007 *Phys. Rev. B* **75** 104110

[125] Gou H, Dubrovinskaia N, Bykova E, Tsirlin A A, Kasinathan D, Schnelle W, Richter A, Merlini M, Hanfl, M, Abakumov A M, Batuk D, Van Tendeloo G, Nakajima Y, Kolmogorov A N and Dubrovinsky L 2013 *Phys. Rev. Lett.* **111** 157002

[126] He X L , Dong X, Wu Q, Zhao Z, Zhu Q, Oganov A R, Tian Y, Yu D, Zhou X F and Wang H T 2018 *Phys. Rev. B* **97** 100102

[127] Kolmogorov A N, Shah S, Margine E R, Bialon A F, Hammerschmidt T and Drautz R 2010 *Phys. Rev. Lett.* **105** 217003

[128] Niu H, Wang J, Chen X Q , Li D, Li Y, Lazar P, Podloucky R and Kolmogorov A N 2012 *Phys. Rev. B* **85** 144116

[129] Zhang M, Lu M, Du Y, Gao L, Lu C and Liu H 2014 *J. Chem. Phys.* **140** 174505

[130] Wang Q, He J, Hu W, Zhao Z, Zhang C, Luo K, Lü Y, Hao C, Lü W, Liu Z, Yu D, Tian Y and Xu B 2015 *J. Materiomics* **1** 45

[131] Li Q, Zhou D, Zheng W, Ma Y and Chen C 2015 *Phys. Rev. Lett.* **115** 185502

[132] Li Q, Zhou D, Zheng W, Ma Y and Chen C 2013 *Phys. Rev. Lett.* **110** 136403

[133] Liang Y, Yuan X and Zhang W 2011 *Phys. Rev. B* **83** 220102

[134] Qin Z, Gong W, Song X, Wang M, Wang H and Li Q 2018 *RSC Adv.* **8** 35664

[135] Romans P A and Krug M P 1966 *Acta Crystallogr.* **20** 313

[136] Zhang R F, Legut D, Lin Z J, Zhao Y S, Mao H K and Veprek S 2012 *Phys. Rev. Lett.* **108** 255502

[137] Zhao Z, Zhou X F , Wang L M , Xu B, He J, Liu Z, Wang H T and Tian Y 2011 *Inorg. Chem.* **50** 9266

[138] Wang X, Bao K, Tian F, Meng X, Chen C, Dong B, Li D, Liu B and Cui T 2010 *J. Chem. Phys.* **133** 044512

[139] Wang X 2012 *J. Chem. Phys.* **137** 184506